Revamping Kaluza-Klein dark matter in an orbifold theory of flavor

Francisco J. de Anda,[1,2,*] Omar Medina,[3,†] José W. F. Valle,[3,‡] and Carlos A. Vaquera-Araujo[4,5,2,§]

[1]*Tepatitlán's Institute for Theoretical Studies, C.P. 47600, Jalisco, México*
[2]*Dual CP Institute of High Energy Physics, C.P. 28045, Colima, México*
[3]*Institut de Física Corpuscular (CSIC-Universitat de València), AHEP Group, Parc Científic de Paterna. C/ Catedrático José Beltrán, 2 E-46980 Paterna (Valencia), Spain*
[4]*Consejo Nacional de Humanidades, Ciencias y Tecnologías, Av. Insurgentes Sur 1582. Colonia Crédito Constructor, Del. Benito Juárez, C.P. 03940, Ciudad de México, México*
[5]*Departamento de Física, DCI, Campus León, Universidad de Guanajuato, Loma del Bosque 103, Lomas del Campestre C.P. 37150, León, Guanajuato, México*

(Received 14 April 2023; accepted 2 August 2023; published 28 August 2023)

We suggest a common origin for dark matter, neutrino mass and family symmetry within the orbifold theory proposed in [Phys. Lett. B **801**, 135195 (2020); Phys. Rev. D **101**, 116012 (2020)]. Flavor physics is described by an A_4 family symmetry that results naturally from compactification. Weakly interacting massive particle dark matter emerges from the first Kaluza-Klein excitation of the same scalar that drives family symmetry breaking and neutrino masses through the inverse seesaw mechanism. In addition to the "golden" quark-lepton mass relation and predictions for $0\nu\beta\beta$ decay, the model provides a good global description of all flavor observables.

DOI: 10.1103/PhysRevD.108.035046

I. INTRODUCTION

Understanding flavor constitutes one of the major challenges in particle physics. Accounting for the observed pattern of fermion masses and the structure of their mixing parameters continues to defy the particle physics community, even more so after the discovery of neutrino oscillations [1–3]. The latter has demonstrated that leptons mix rather differently from the way quarks do in the Cabibbo–Kobayashi–Maskawa (CKM) model. The Standard Model lacks a symmetry-based organizing principle that one may use to describe flavor properties. The striking oddness of the fermion pattern is unlikely to result just from randomness. Rather, it indicates the presence of some "family" or "flavor" symmetry, a compilation of possibilities for discrete non-Abelian groups as family symmetry candidates is given in [4].

The existence of extra space-time dimensions may shed light on the two complementary aspects of the flavor problem. Indeed, while mass hierarchies may result from geometry [5], mixing angle relations may be predicted from adequate symmetries [6,7], thereby covering both sides of the coin.

Here we focus on six-dimensional orbifold theories proposed in [8,9]. In contrast to the warped flavordynamics picture suggested in [6,7], where family symmetries were imposed by hand, here an A_4 family symmetry results naturally from compactification, a setup that was first introduced and described in detail in references [10–12]. Dark matter emerges as the first Kaluza-Klein (KK) excitation of the same scalar that drives lepton number violation, and family symmetry breakdown, leading to neutrino masses through an inverse seesaw mechanism. This new seed scalar field allows us to resurrect the KK dark matter proposal. The model leads naturally to the "golden" quark-lepton mass relation, that implies strong predictions for the light-quark masses m_d and m_s and neutrinoless double beta decay. It also provides an adequate description of neutrino oscillation parameters, together with a very good global description of flavor observables.

This letter is structured as follows. In Sec. II we recapitulate the theory framework of our model, while in Sec. III we describe the general features of Kaluza-Klein dark matter, followed in Sec. IV by an analysis of the phenomenology of σ^{KK} as a WIMP dark matter candidate. In Sec. V we present the "golden quark-lepton" mass formula, results for the neutrino sector, and also discuss our global fit to flavor observables. In Sec. VI we

*fran@tepaits.mx
†Omar.Medina@ific.uv.es
‡valle@ific.uv.es
§vaquera@fisica.ugto.mx

present a brief summary and additional discussion of our model.

II. THEORY FRAMEWORK

Our model is a 6-dimensional version of the Standard Model implementing the inverse seesaw mechanism [13,14]. It provides is a simple extension of the model presented in [8], where the orbifold compactification implies a discrete A_4 family symmetry in four dimensions [10–12,15]. We stress that the 4-dimensional flavor symmetry is not arbitrary, but rather dictated by the extra-dimensional symmetries of our construction. We assume a sequential setup where 3 singlet fermions S accompany the 3 "right-handed" neutrinos. The transformation properties of the fields under the gauge and family symmetry and their localization on the orbifold are shown in Table I.

The scalar sector consists of three Higgs doublets H_u, H_d and H_ν plus an extra singlet scalar σ, all transforming as flavor triplets. Given the auxiliary discrete symmetries $\mathbb{Z}_3$ and $\mathbb{Z}_4$ in Table I, H_d only couples to down type fermions (charged leptons and down quarks), while H_u couples only to up quarks and H_ν only couples to neutrinos. The effective Yukawa terms are given by

$$\begin{aligned}\mathcal{L}_Y = {} & y_1^\nu (L H_\nu \nu^c)_1 + y_2^\nu (L H_\nu \nu^c)_2 + \frac{y^S}{2}\sigma S S + m_{\nu^c S}\nu^c S \\ & + y_1^d (Q d^c H_d)_1 + y_2^d (Q d^c H_d)_2 + y_1^e (L e^c H_d)_1 \\ & + y_2^e (L e^c H_d)_2 + y_1^u (Q H_u)_{1'} u_1^c + y_2^u (Q H_u)_{1''} u_2^c \\ & + y_3^u (Q H_u)_1 u_3^c, \end{aligned} \tag{1}$$

where $()_{1,2}$ and $()_{1,1',1''}$ indicate possible singlet contractions $\mathbf{3}\times\mathbf{3}\times\mathbf{3}\to\mathbf{1}_{1,2}$ and $\mathbf{3}\times\mathbf{3}\to\mathbf{1}_{1,1',1''}$ in A_4. Here we will also assume all dimensionless Yukawa couplings to be real.

Moreover, we adopt a dynamical scenario where lepton number and family symmetries are violated spontaneously, through the expectation value of an extra scalar field σ, whose vacuum expectation value (VEV) yields Majorana masses to the singlet fermion S. The VEV of σ must lie in the zero mode of the extra dimensional field decomposition [16], and must comply with the $\mathbb{Z}_2$ boundary condition

$$P\langle\sigma\rangle = \langle\sigma\rangle. \tag{2}$$

Here P defines an arbitrary gauge twist of the orbifold, associated to its geometry, and is chosen to be

$$P = \frac{1}{3}\begin{pmatrix} -1 & 2\omega^2 & 2\omega \\ 2\omega & -1 & 2\omega^2 \\ 2\omega^2 & 2\omega & -1 \end{pmatrix}, \tag{3}$$

with $\omega = e^{2\pi i/3}$, the cube root of unity. Notice that it satisfies $P^2 = 1$. This boundary condition aligns the VEV as

$$\langle\sigma\rangle = v_\sigma \begin{pmatrix} 1 \\ \omega \\ \omega^2 \end{pmatrix}, \tag{4}$$

The Higgs doublets are assumed to obtain the most general vacuum alignment, which we parametrize as in [8], these alignments require in general A_4 soft breaking terms in the scalar potential [17,18], nonetheless they are a possibility for obtaining viable neutrino mixing results in models with three Higgs-doublets as an A_4 triplet [19],

$$\begin{aligned} \langle H_u\rangle &= v_u \begin{pmatrix} \epsilon_1^u e^{i\phi_1^u} \\ \epsilon_2^u e^{i\phi_2^u} \\ 1 \end{pmatrix}, \qquad \langle H_\nu\rangle = v_\nu e^{i\phi^\nu} \begin{pmatrix} \epsilon_1^\nu e^{i\phi_1^\nu} \\ \epsilon_2^\nu e^{i\phi_2^\nu} \\ 1 \end{pmatrix}, \\ \langle H_d\rangle &= v_d e^{i\phi^d} \begin{pmatrix} \epsilon_1^d e^{i\phi_1^d} \\ \epsilon_2^d e^{i\phi_2^d} \\ 1 \end{pmatrix}. \end{aligned} \tag{5}$$

The explicit form of the mass matrices for the quarks and charged leptons (up to unphysical rephasings) is given as

$$\begin{aligned} M_u &= v_u \begin{pmatrix} y_1^u\epsilon_1^u & y_2^u\epsilon_1^u & y_3^u\epsilon_1^u \\ y_1^u\epsilon_2^u\omega^2 & y_2^u\epsilon_2^u\omega & y_3^u\epsilon_2^u \\ y_1^u\omega & y_2^u\omega^2 & y_3^u \end{pmatrix}, \\ M_d &= v_d \begin{pmatrix} 0 & y_1^d\epsilon_1^d e^{i(\phi_1^d-\phi_2^d)} & y_2^d\epsilon_2^d \\ y_2^d\epsilon_1^d e^{i(\phi_1^d-\phi_2^d)} & 0 & y_1^d \\ y_1^d\epsilon_2^d & y_2^d & 0 \end{pmatrix}, \\ M_e &= v_d \begin{pmatrix} 0 & y_1^e\epsilon_1^d e^{i(\phi_1^d-\phi_2^d)} & y_2^e\epsilon_2^d \\ y_2^e\epsilon_1^d e^{i(\phi_d^1-\phi_2^d)} & 0 & y_1^e \\ y_1^e\epsilon_2^d & y_2^e & 0 \end{pmatrix}, \end{aligned} \tag{6}$$

Turning now to the neutral fermion mass matrix, in the (ν, ν^c, S) basis, it is given as

TABLE I. Field content of the model.

Field	$SU(3)_C$	$SU(2)_L$	$U(1)_Y$	A_4	$\mathbb{Z}_3$	$\mathbb{Z}_4$	Localization
L	$\mathbf{1}$	$\mathbf{2}$	$-1/2$	$\mathbf{3}$	1	1	Brane
d^c	$\bar{\mathbf{3}}$	$\mathbf{1}$	$1/3$	$\mathbf{3}$	1	1	Brane
e^c	$\mathbf{1}$	$\mathbf{1}$	1	$\mathbf{3}$	1	1	Brane
Q	$\mathbf{3}$	$\mathbf{2}$	$1/6$	$\mathbf{3}$	1	1	Brane
$u^c_{1,2,3}$	$\bar{\mathbf{3}}$	$\mathbf{1}$	$-2/3$	$\mathbf{1''},\mathbf{1'},\mathbf{1}$	ω	1	Bulk
ν^c	$\mathbf{1}$	$\mathbf{1}$	0	$\mathbf{3}$	ω^2	i	Brane
S	$\mathbf{1}$	$\mathbf{1}$	0	$\mathbf{3}$	ω	$-i$	Brane
H_u	$\mathbf{1}$	$\mathbf{2}$	$1/2$	$\mathbf{3}$	ω^2	1	Brane
H_d	$\mathbf{1}$	$\mathbf{2}$	$-1/2$	$\mathbf{3}$	1	1	Brane
H_ν	$\mathbf{1}$	$\mathbf{2}$	$1/2$	$\mathbf{3}$	ω	$-i$	Brane
σ	$\mathbf{1}$	$\mathbf{1}$	0	$\mathbf{3}$	ω	-1	Bulk

$$M_\nu = \begin{pmatrix} 0 & M_D & 0 \\ M_D^T & 0 & M_{\nu^c S} \\ 0 & M_{\nu^c S}^T & M_S \end{pmatrix}, \tag{7}$$

with

$$M_D = v_\nu \begin{pmatrix} 0 & y_1^\nu \epsilon_1^\nu e^{i(\phi_1^\nu - \phi_2^\nu)} & y_2^\nu \epsilon_2^\nu \\ y_2^\nu \epsilon_1^\nu e^{i(\phi_1^\nu - \phi_2^\nu)} & 0 & y_1^\nu \\ y_1^\nu \epsilon_2^\nu & y_2^\nu & 0 \end{pmatrix},$$

$$M_{\nu^c S} = m_{\nu^c S} \begin{pmatrix} 1 & 0 & 0 \\ 0 & 1 & 0 \\ 0 & 0 & 1 \end{pmatrix},$$

$$M_S = y^S v_\sigma \begin{pmatrix} 0 & \omega^2 & \omega \\ \omega^2 & 0 & 1 \\ \omega & 1 & 0 \end{pmatrix}. \tag{8}$$

After spontaneous symmetry breaking, the light neutrinos acquire masses through the inverse seesaw mechanism, characterized by the effective mass matrix [13,14]

$$m_\nu \sim M_D M_{\nu^c S}^{-1} M_S M_{\nu^c S}^{T-1} M_D^T = \frac{M_D M_S M_D^T}{m_{\nu^c S}^2}. \tag{9}$$

Notice that, due to the family symmetry, the singlet mass entry $\nu^c S$ is trivial and the others, M_D and M_S, have zeros along the diagonal. We will assume the following hierarchy of scales

$$M_D \sim \langle H_\nu \rangle \sim \mathcal{O}(\text{GeV}), \qquad M_S \sim \langle \sigma \rangle \lesssim \mathcal{O}(\text{GeV}),$$
$$m_{\nu^c S} \sim \mathcal{O}(10\ \text{TeV}). \tag{10}$$

This choice renders naturally light neutrino masses.

III. REVAMPING KALUZA-KLEIN DARK MATTER

Besides the gauge fields, our model contains only two fields that propagate into the bulk, namely u_i^c and σ, where the latter is an electrically neutral scalar transforming as a singlet under the symmetries of the $SU(3)_c \otimes SU(2)_L \otimes U(1)_Y$ gauge group. In this section we examine the possibility of identifying the lightest Kaluza-Klein mode of σ as a WIMP dark matter candidate.

The extra dimensions are orbifolded by a $\mathbb{Z}_2$. Every field has a different $\mathbb{Z}_2$ charge, depending on its A_4 and Lorentz transformation. In principle, one could choose the charge for each field individually, which implies that some couplings are also charged under the $\mathbb{Z}_2$ orbifolding, usually called kink couplings. We instead assume that each coupling constant in the model is trivial under orbifolding. This leaves the $\mathbb{Z}_2$ orbifolding symmetry as a symmetry of the compactified Lagrangian. This surviving $\mathbb{Z}_2$ (not to be confused with the discrete auxiliary symmetry in Table I) protects the lightest KK mode, making it stable and a potential dark matter candidate.

In order to determine the mass scale of the lightest KK mode, we start by analyzing the spectrum of the effective 4-dimensional theory that emerges after the $T^2/\mathbb{Z}_2$ orbifold compactification of the extra two dimensions present in our construction. Denoting the extra dimensions by a single complex coordinate z, we can decompose any field in the bulk Ψ (fermion, scalar or vector) into a tower of low-energy 4-dimensional effective modes $\Psi_{ni}(x)$ as

$$\Psi(x,z) = \sum_{n,m=-\infty}^{\infty} \sum_{i=\pm} \Psi_{nmi}(x) f_{nmi}(z), \tag{11}$$

where the profiles $f_{ni}(z)$ are eigenfunctions of the extra dimensional translation and the $\mathbb{Z}_2$ orbifold parity, these satisfy by definition the following conditions

$$f_{nm\pm}(z) = f_{nm\pm}(z+1) = f_{nm\pm}(z+\omega) = \pm f_{nm\pm}(-z). \tag{12}$$

To obtain a more explicit expression of the profiles, we use the definition of the complex coordinate z on the torus;

$$z = (y_5 + \omega y_6)/2\pi R, \tag{13}$$

where $\omega = -1/2 + i\sqrt{3}/2$, and each real coordinate $y_{5,6}$ runs through each fundamental circle that generates the torus. Thus, given the conditions in Eq. (12), we find that the eigenfunctions can be written as

$$f_{nm}(z) \sim e^{i(ny_5 + my_6)/R} = e^{2i\pi \text{Re}z[n(1-i/\sqrt{3}) - 2im/\sqrt{3}]}, \tag{14}$$

up to a normalization constant. From these, we can build the parity eigenfunctions

$$f_{nm+}(z) = \frac{f_{nm}(z) + f_{nm}(-z)}{\sqrt{2}},$$
$$f_{nm-}(z) = \frac{f_{nm}(z) - f_{nm}(-z)}{i\sqrt{2}}, \tag{15}$$

which are orthonormal functions [20], satisfying

$$\int dz dz^* f_{nmi}(z) f_{n'm'i'}(z) = \delta^n_{n'} \delta^m_{m'} \delta^i_{i'}. \tag{16}$$

As a result of the periodicity conditions in Eq. (12) and orthonormality from Eq. (16), the profiles must be translation eigenfunctions (which for flat extra dimensions are exponentials) with

$$\partial_z f_{nmi} = M_{nmi} f_{nmi}, \tag{17}$$

with M_{nmi} proportional to $M_{nmi} \sim 1/R$ where R is the compactification scale. Hence, for example, the kinetic term for a 6-dimensional scalar field becomes a collection of mass terms for their corresponding 4-dimensional effective degrees of freedom

$$\begin{aligned}\int dz dz_0 (\partial_z \Psi)^\dagger \partial_z \Psi &= \sum_{n,n',m,m',i,i'} M_{nmi} M_{n'm'i'} \Psi^\dagger_{nmi} \Psi_{n'm'i'} \\ &\times \int dz dz_0 f^*_{nmi} f_{n'm'i'} \\ &= \sum_{n,m,i} M^2_{nmi} \Psi^\dagger_{nmi} \Psi_{nmi}, \end{aligned} \tag{18}$$

with an analogous relation for fermions. By choosing an orthonormal basis, the KK modes are already in the mass basis. Note that the zero-mode has an eigenvalue $M_{0i} = 0$, so that its profile $f_{0i} \equiv f_0$ is a constant. The zero-modes remain massless after compactification, and can be identified at low energies with the SM fields.

Concerning the heavy KK modes, there is an important result that comes from the preservation of the orbifolding $\mathbb{Z}_2$ symmetry. If one tries to build a term involving a single heavy KK mode Ψ_{nj} (with $n \geq 1$) and any number N of massless zero modes $\Psi^{(k)}_0$, $k = 1, \ldots, N$, one finds that such term automatically vanishes, as the effective 4-dimensional coupling comes from integrating the extra dimensional profiles

$$\begin{aligned}&\int dz dz_0 \Psi^{(1)}_0 \cdot \ldots \cdot \Psi^{(N)}_0 \Psi_{nmj} f^N_0 f_{nmj} \\ &= \Psi^{(1)}_0 \cdot \ldots \cdot \Psi^{(N)}_0 \Psi_{nmj} f^{N-1}_0 \int dz dz_0 f_0 f_{nmj} \\ &= \Psi^{(1)}_0 \cdot \ldots \cdot \Psi^{(N)}_0 \Psi_{nmj} f^{N-1}_0 \delta^n_0 \delta^m_0 = 0. \end{aligned} \tag{19}$$

The first line follows from the fact that the Ψ functions do not depend on the extra dimensions, and the zero mode profiles are just a constant. The second line results from the orthonormality of the profiles. Such terms would in general induce the decay of KK modes into N massless modes. However, in our construction these terms clearly do not exist. There might be destabilizing interactions between KK modes. However, only the "right-handed" up-type quarks u^c and the σ scalar have KK modes, and these do not interact with each other. Therefore these do not generate destabilizing interactions. Another possible origin of destabilization could come from the interaction between the KK mode $\Psi(x,z) = \Psi_{nmi}(x) f_{nmi}(z)$ and a generic brane-localized field $\Phi(x,z) = \Phi(x)\delta(z - z_0)\delta(\bar{z} - \bar{z}_0)$, where the branes lie at the fixed points of the orbifold [8,11,12,15] labeled by z_0,

$$z_0 \in \left\{0, \frac{1}{2}, \frac{\omega}{2}, \frac{\omega^2}{2}\right\}. \tag{20}$$

These interactions have the form

$$\begin{aligned}&\int dz d\bar{z} \Psi_{nmi}(x) \Phi(x) f_{nmi}(z) \delta(z - z_0) \delta(\bar{z} - \bar{z}_0) \\ &= \Psi_{nmi}(x) \Phi(x) f_{nmi}(z_0), \end{aligned} \tag{21}$$

we can use Eq. (15) to rewrite the parity eigenfunctions as

$$\begin{aligned} f_{nm+}(z) &\sim \cos\left(2\pi \mathrm{Re} z[n(1 - i/\sqrt{3}) - 2im/\sqrt{3}]\right), \\ f_{nm-}(z) &\sim \sin\left(2\pi \mathrm{Re} z[n(1 - i/\sqrt{3}) - 2im/\sqrt{3}]\right). \end{aligned} \tag{22}$$

From the last equation we can see that the negative parity profile vanishes at any of the four fixed points

$$f_{nm-}(z_0) = 0, \tag{23}$$

due to the parity identification, as can be easily checked by direct calculation. Consequently to have a stable DM candidate in the model we assume that the lightest KK mode has negative parity and thus has no brane interactions with the SM fields in the 4-D theory that could destabilize it.

In the present model there are three types of fields in the bulk, the gauge fields, the right-handed up-type quarks u^c and the σ scalar driving lepton number and family symmetry breaking. In the following we will assume that the lightest KK mode is electrically neutral. That leaves us with the first KK modes of the neutral SM gauge bosons: the photon, gluon or the Z boson [21], as well as first KK mode of the σ scalar. The latter is charged only under A_4 and drives family symmetry breaking and neutrino mass generation. The lightest KK excitation of this field is a potential dark matter candidate. After orbifold compactification and spontaneous electroweak symmetry breaking the first neutral KK modes will acquire masses of the order

$$\begin{aligned} M^2_{(\gamma,g)^{KK}} &\sim \left(\frac{1}{2R}\right)^2, \qquad M^2_{Z^{KK}} \sim \left(\frac{1}{2R}\right)^2 + m^2_Z, \\ M^2_{\sigma^{KK}} &\sim \left(\frac{1}{2R}\right)^2 + m^2_\sigma. \end{aligned} \tag{24}$$

In the simplest extra dimensional extension of the SM it is natural to assume that the lightest KK particle (LKP) is the first mode of the photon or the gluon, as their zero mode always remains massless.

Note that Eq. (24) only gives the order of magnitude of the first excitations, any mass hierarchy can be assumed for the neutral KK light modes. If one assumes that the LKP is a dark matter candidate and identifies it with the first excitation of the photon, the gluon or the Z gauge boson, it is in general difficult to successfully reproduce the observed dark matter relic abundance, since the all gauge couplings are completely fixed, their masses being the only free parameter, determined by the compactifcation scale.

In particular, if the first KK mode of the photon is identified with the LKP, in order to correctly reproduce the required relic abundance a mass of order $M_{(\gamma,Z)^{KK}} \sim 1$ TeV is required [22,23]. Similarly, if the LKP is the first KK gluon then its mass must be of order $M_{g^{KK}} \sim 5$ TeV [24]. Note that both scenarios predict compactification scales that lie in tension the LEP bound in Eq. (25). Furthermore, the case of vector dark matter is currently disfavored experimentally [25].

Previous proposals [21–24] with the LKP as a dark matter candidate, assumed the LKP to be associated to a Standard Model field, a possibility no longer viable experimentally. In our present setup, the LKP comes from a genuinely new field, beyond those of the Standard Model. This field drives lepton number violation, and plays a key role in explaining the flavor structure of the fermions [8,9]. This choice is not only well-motivated but also relaxes the constraints, allowing us to build a viable and predictive model. Indeed, we will show that if the first KK mode of σ is identified with the LKP it can play the role of a WIMP dark matter candidate.

Before closing this section, we comment on the key role played by the compactification scale on the Kaluza-Klein WIMP dark matter phenomenology. It has long been noted that the existence of a KK tower generates flavor changing neutral currents (FCNCs). These arise when the extra-dimensional fields in the bulk are allowed to have an explicit mass term, which prevents the simultaneous flavor diagonalization of their higher KK modes with the zeroth level Lagrangian [26,27]. We note, however, that our model is built in six flat dimensions, and the bulk fermions are 6-D chiral fields, with no explicit mass terms. As a result, it is free from FCNCs of this kind by construction. However, an important effect arises from the additional contributions to the electroweak precision observables. The Peskin-Takeuchi S, T and U parameters are modified by the existence of a tower of massive vector $SU(2)_L$ triplets. The current experimental bound for a setup with 2 flat non-universal extra dimensions is [28,29]

$$\frac{1}{2R} \gtrsim 2.1 \text{ TeV}. \tag{25}$$

As shown in Eq. (24), the mass of the first neutral KK mode for σ has two contributions. The first one comes from the compactification scale constrained above. The second contribution m_σ^2 is actually negative, since the zero-mode σ must develop a VEV $\langle\sigma\rangle$ after spontaneous symmetry breaking. This triggers neutrino mass generation by the inverse seesaw mechanism [13,14] and breaks the family symmetry as well. Its associated scale $\langle\sigma\rangle$ is estimated in Eq. (10). As we will show in the next section the model can accommodate naturally a mass of a few TeV for the LKP, which can provide a viable WIMP dark matter particle.

IV. σ^{KK} AS A VIABLE WIMP DARK MATTER CANDIDATE

Here we show how the lightest KK mode of the field σ, identified as the LKP, can be a successful WIMP dark matter candidate, while the corresponding scalar simultaneously provides small neutrino masses through a low-scale inverse seesaw mechanism [13,14], and the breakdown of a flavour symmetry following the lines proposed in [8,9].

In our model the complex scalar singlet σ transforms as a triplet under the A_4 flavor symmetry, providing the source of A_4 flavor symmetry breaking, driving low-scale neutrino mass generation through spontaneous violation of lepton number. We now discuss the role of the first KK mode of σ as a DM candidate in our framework. In contrast to the case of the gauge bosons, its couplings are not fixed by SM interactions. As a result they can be used to fit the observed relic abundance and direct detection constraints [24], together with a viable compactification scale and a natural mechanism for light neutrino masses.

After compactification, one obtains a 4-dimensional scalar potential whose relevant terms can be written generically as

$$\begin{aligned}\mathcal{L}_\sigma = {} & \mu_\sigma^2 \sigma^\dagger \sigma + \lambda_\sigma (\sigma^\dagger \sigma)^2 + \tilde{\lambda}_\sigma (\sigma^\dagger \sigma \sigma^\dagger \sigma) \\ & + \lambda_{u,d,\nu} \sigma^\dagger \sigma H_{u,d,\nu}^\dagger H_{u,d,\nu}.\end{aligned} \tag{26}$$

In the above relation, the λ_σ term involves the $3 \times 3 \to 1$ contraction under the A_4 symmetry, while the $\tilde{\lambda}_\sigma$ term characterizes the symmetric $3 \times 3 \times 3 \times 3 \to 1$ contraction. As stated in the previous section, the lightest KK mode must have negative parity in order to vanish at the branes, making it a stable DM candidate. Equation (26) shows that the effective Lagrangian below the compactification scale does have the $\lambda_{u,d,\nu}$ term. This term is absent at tree level, but is generated radiatively at one loop, mediated by the KK modes of the σ field. The coefficient μ_σ^2 is negative, in consistency with the spontaneous symmetry breakdown driven by the zero mode of σ. The corresponding VEV becomes

$$v_\sigma^2 = \frac{-\mu_\sigma^2}{2\lambda_\sigma + 6\tilde{\lambda}_\sigma}, \tag{27}$$

where we have assumed that the alignment of σ is fixed by the extra dimensional boundary condition, entering as an input to the potential [16]. Note that the scale of v_σ is determined by the arbitrary parameter μ_σ^2 which is unrelated to the compactification scale. An important consequence of the spontaneous symmetry breaking is that Eq. (24) is rewritten as

$$M_{\sigma^{KK}}^2 \sim \left(\frac{1}{2R}\right)^2 + \mu_\sigma^2, \tag{28}$$

with $\mu_\sigma^2 < 0$, which allows the first excited mode of σ to be identified as the LKP and, as we will see, implement the WIMP dark matter picture.

We can further improve the estimate for the LKP mass by decomposing a generic bulk field into an infinite tower of orbifold eigenstates, as shown in Eq. (11). Each 6-dimensional field should be decomposed into a series of the extra dimensional translation and reflection eigenstates For example the bulk σ field, which is a flavor triplet, should be decomposed as a linear combination of the three eigenvectors of the boundary condition matrix in Eq. (3). Therefore, its full decomposition into orbifold eigenstates is

$$\sigma(x,z) = \sum_{n,m=0}^{\infty} \left[\sigma_{nm+}(x) \frac{1}{\sqrt{3}} \begin{pmatrix} 1 \\ \omega \\ \omega^2 \end{pmatrix} f_{n+}(z) + \sigma_{nm-}(x) \frac{1}{\sqrt{2}} \begin{pmatrix} 1 \\ 0 \\ -\omega^2 \end{pmatrix} f_{n-}(z) + \tilde{\sigma}_{nm-}(x) \frac{1}{\sqrt{2}} \begin{pmatrix} 0 \\ 1 \\ -\omega \end{pmatrix} f_{n-}(z) \right], \tag{29}$$

where the three 4-dimensional towers of fields $\sigma_{nm+}, \sigma_{nm-}$, $\tilde{\sigma}_{nm-}$ represent the components of the A_4 triplet. Here the labels $\pm$ denote the eigenvectors corresponding to the ± 1 eigenvalues of the extra dimensional boundary condition in Eq. (3). In this notation, the zero mode is associated with a constant profile f_{0+} and a vanishing f_{0-}. The LKP would correspond to the first mode, which can be any of the two negative parity complex scalars

$$\sigma_{1LKP} = \sigma_{1-}(x) \frac{1}{\sqrt{2}} \begin{pmatrix} 1 \\ 0 \\ -\omega^2 \end{pmatrix}, \qquad \sigma_{2LKP} = \tilde{\sigma}_{1-}(x) \frac{1}{\sqrt{2}} \begin{pmatrix} 0 \\ 1 \\ -\omega \end{pmatrix}. \tag{30}$$

Due to the orbifolding, and the fact that they form a triplet under the A_4 symmetry, these obtain the same mass $\sim 1/(2R)$ after compactification. The degeneracy is lifted by the potential due to the zero mode VEV v_σ However, under the natural assumption $1/(2R) \gg v_\sigma$, the mass splitting is expected to be small. From the scalar potential in Eq. (26) we can obtain the mass contributions arising from v_σ as

$$\mathcal{L}_{m\sigma} = (\sigma_{1+}^*, \sigma_{1-}^*, \tilde{\sigma}_{1-}^*) \begin{pmatrix} \frac{1}{4R^2} - (5\lambda_\sigma + 7\tilde{\lambda}_\sigma) v_\sigma^2 & 0 & 0 \\ 0 & \frac{1}{4R^2} - \frac{10\lambda_\sigma + 11\tilde{\lambda}_\sigma}{2} v_\sigma^2 & -\frac{5\omega^2\lambda_\sigma + (2-\omega-5\omega^2)\tilde{\lambda}_\sigma}{2} v_\sigma^2 \\ 0 & -\frac{5\omega\lambda_\sigma + (2-\omega^2-5\omega)\tilde{\lambda}_\sigma}{2} v_\sigma^2 & \frac{1}{4R^2} - \frac{10\lambda_\sigma + 11\tilde{\lambda}_\sigma}{2} v_\sigma^2 \end{pmatrix} \begin{pmatrix} \sigma_{1+} \\ \sigma_{1-} \\ \tilde{\sigma}_{1-} \end{pmatrix}. \tag{31}$$

From the mass matrix, one can see that for $\lambda_\sigma, \tilde{\lambda}_\sigma > 0$ the negative parity modes (σ_{1-}, and $\tilde{\sigma}_{1-}$) are naturally the lightest, as required so that one of them is the DM candidate.

Barring the presence of new annihilation and co-annihilation channels, the parameter space allowed by the observed relic complex-scalar dark matter abundance and direct detection is in general very constrained [30]. In our model the parameter space is widened by the fact that the KK modes are nearly degenerate in mass, leading naturally to a multicomponent dark matter picture. The underlying mechanism responsible for this widening of the parameter space involves the presence of multiple scalars, which introduce new annihilation and co-annihilation channels in the Higgs-portal scenario. These channels go beyond the conventional s-channel mediated by the Higgs boson, including one of the dark scalars in the t-channel, as well as co-annihilation processes involving two dark scalars and two Higgs bosons. These additional channels can produce the correct relic abundance of dark matter while alleviating tensions arising from direct detection searches. Moreover, the widening effect is more pronounced when the mass difference between the dark scalars is small, which is natural in our model, as discussed above [31].

In order to demonstrate the viability of our model as a theory for dark matter, it suffices to consider a simplified scenario in which all the non-SM fields are heavy and decouple, except for the almost degenerate complex scalars σ_{1+}, σ_{1-} and $\tilde{\sigma}_{1-}$. For illustration we will include only one Higgs doublet H, omitting the explicit A_4 contractions. Note that the implementation of the A_4 symmetry introduces a total of 9 Higgs doublets, making the scalar sector significantly richer than that of the SM. However, after the A_4 symmetry is spontaneously broken, the model effectively yields the SM with an enlarged scalar sector. This simplified scenario can be seen as a worst case-scenario where only one Higgs scalar is the mediator of DM annihilation. After spontaneous symmetry breaking this simplified DM model coincides with our complete A_4 model in the limit in which the extra Higgs fields are much heavier than the SM 125 GeV Higgs and effectively

decouple. This way the relevant Higgs portal parameters are the effective quartic coupling constants of the extended scalar sector characterizing the potential

$$V(H,\sigma_{1-},\tilde{\sigma}_{1-}) \supset \lambda_1 H^\dagger H \sigma^*_{1+}\sigma_{1+} + \lambda_2 H^\dagger H \sigma^*_{1-}\sigma_{1-} + \lambda_3 H^\dagger H \tilde{\sigma}^*_{1-}\tilde{\sigma}_{1-} + \lambda_4 H^\dagger H(\tilde{\sigma}^*_{1-}\sigma_{1-} + \sigma^*_{1-}\tilde{\sigma}_{1-}). \quad (32)$$

From the above discussion, the quartic coupling constants in this simplified potential emerge from the $\lambda_{u,d,\nu}$ couplings of Eq. (26) after A_4 spontaneous symmetry breaking. Note that there is no $\sigma_+\sigma_-$ mixing, as there is a remnant $\mathbb{Z}_2$ orbifolding parity which is preserved by the original Lagrangian and also by the effective radiatively generated Lagrangian.

In order to ensure perturbativity we have studied the relic abundance and direct detection constraints for this simplified scenario. We have varied randomly the relevant parameters in the range $0 < \lambda_i < \sqrt{4\pi}$. Moreover, we have modeled a small mass splitting among the three physical scalars identifying ϕ_1, a linear combination of σ_{1-} and $\tilde{\sigma}_{1-}$ as the LKP dark matter candidate, and scanning the mass parameters within the range $0 < m_{\phi_1} = m_{\rm DM} < 10^4$ GeV, $m_{\rm DM} < m_{\phi_2}, m_{\sigma_{1+}} < 1.2 \times m_{\rm DM}$.

The results are shown in Fig. 1. Each magenta point corresponds to a model parameter combination that reproduces the correct relic abundance $\Omega h^2 = 0.120$ [32] through Higgs portal interactions, and enhanced by rescattering with the other nearly degenerate complex scalars in the first KK-mode sector [31]. This way the model opens a rather large parameter window below the current direct detection constraints, including the recent ones of LUX-ZEPLIN [33]. Many of these points will be probed within upcoming dark matter experiments. [34–36]

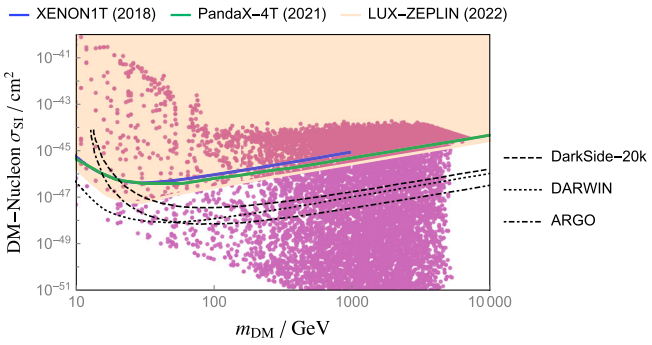

FIG. 1. The direct detection and relic abundance constraints versus the dark matter mass $m_{\rm DM} = m_{\phi_1}$. Each magenta point corresponds to a combination of the model parameters that give the correct relic abundance $\Omega h^2 = 0.120$. The orange shaded region is ruled out by the LUX-ZEPLIN experiment [33]. We also show the PandaX-4T [37] and XENON1T [38] limits, and the projected sensitivities of some upcoming direct detection experiments [34–36].

In conclusion we find that our LKP, the lightest complex scalar contained in the first excited mode of σ, can provide a viable WIMP dark matter candidate.

V. FLAVOR PREDICTIONS AND GLOBAL FIT

Our model is based on an $A_4 \otimes \mathbb{Z}_3 \otimes \mathbb{Z}_4$ family symmetry as summarized in Table I, with a total of 17 independent parameters that determine the flavor properties of both the quark and lepton sectors. These parameters, described in Eqs. (1)–(8), can be written compactly as

$$\left\{ (y^\nu_{1,2} v_\nu) \frac{\sqrt{y^S v_\sigma}}{m_{\nu^c S}}, y^{e,d}_{1,2} v_d, y^u_{1,2,3} v_u, \epsilon^{u,\nu,d}_{1,2}, \phi^{\nu,d}_1 - \phi^{\nu,d}_2 \right\}. \quad (33)$$

We have performed a goodness of fit analysis of the model using a reduced chi-squared test. The reference values for the flavor related observables for the quark and lepton sectors were taken from references [3,39,40], and the masses of the SM fermions were taken at the Z-boson mass (M_Z) scale.

Our chi-square test assesses how well the model is able to describe the 19 experimentally determined low-energy flavor observables, including the SM fermion masses, the quark mixing parameters, and the neutrino oscillation parameters,

$$\{m_{u,c,t,d,s,b,e,\mu,\tau}, \Delta m^2_{21}, \Delta m^2_{31}, \theta^q_{12,13,23}, \theta^\ell_{12,13,23}, \delta^q, \delta^\ell\}, \quad (34)$$

therefore the number of degrees of freedom $K = 19 - 17 = 2$.

Table II summarizes the results from our goodness-of-fit global analysis of flavor observables. There are some features of this work that we would like to stress. For the lepton sector the analysis was performed using the updated values for the neutrino oscillation parameters, given in the neutrino global fit of Ref. [3], in contrast to the previous works [8,9]. Moreover, this model employs a low-scale seesaw mechanism, i.e. the inverse seesaw, instead of the high-scale type-I seesaw mechanism. The light-neutrino masses are generated in a very different way, leading to quantitative differences between the present model and previous variants. This becomes very transparent by noting that the viable $0\nu\beta\beta$ decay region in this work (see Fig. 3) is quite different from those in previous studies. The values for the different charged lepton masses are taken from [39]. For the quark masses we used an updated determination from Ref. [40]. For definiteness we assume the experimentally preferred case of normal ordered (NO) neutrino spectrum. Our best fit point, as described in detail by Table II, yields $\chi^2_K = \frac{\chi^2}{K} = 1.05$,

TABLE II. Summary of our goodness-of-fit global analysis of flavor observables. Charged lepton masses are taken from [39] and quark masses are based on [40]. Neutrino oscillation parameters are taken from [3] assuming normal-ordering.

Parameter	Value
$y_1^e v_d/\text{GeV}$	1.746
$y_2^e v_d/(10^{-1}\ \text{GeV})$	−9.78
$y_1^d v_d/\text{GeV}$	−2.85
$y_2^d v_d/(10^{-2}\ \text{GeV})$	−7.35
$(y_1^\nu v_\nu)\sqrt{y^S v_\sigma}/(m_{\nu^c S}\ \sqrt{\text{eV}})$	0.081
$(y_2^\nu v_\nu)\sqrt{y^S v_\sigma}/(m_{\nu^c S}\ \sqrt{\text{eV}})$	−0.017
$y_1^u v_u/(10^{-3}\ \text{GeV})$	−4.765
$y_2^u v_u/(10^{-1}\ \text{GeV})$	3.582
$y_3^u v_u/\text{GeV}$	−7.08
$\epsilon_1^u/10^{-2}$	−8.65
ϵ_2^u	23.7
$\epsilon_1^d/10^{-2}$	1.80
$\epsilon_2^d/10^{-4}$	9.12
ϵ_1^ν	1.749
ϵ_2^ν	−7.397
$(\phi_1^d - \phi_2^d)/\pi$	−0.076
$(\phi_1^\nu - \phi_2^\nu)/\pi$	−0.321

	Data		
Observable	Central value	1σ range	Model best fit
$\sin^2\theta_{12}^\ell/10^{-1}$	3.18	$3.02 \to 3.34$	3.18
$\sin^2\theta_{13}^\ell/10^{-2}$ (NO)	2.200	$2.138 \to 2.269$	2.199
$\sin^2\theta_{23}^\ell/10^{-1}$ (NO)	5.74	$5.60 \to 5.88$	5.74
δ^ℓ/π (NO)	1.08	$0.96 \to 1.21$	1.12
m_e/MeV	0.486	$0.486 \to 0.486$	0.486
m_μ/GeV	0.102	$0.102 \to 0.102$	0.102
m_τ/GeV	1.746	$1.746 \to 1.746$	1.746
$\Delta m_{21}^2/(10^{-5}\ \text{eV}^2)$	7.50	$7.30 \to 7.72$	7.50
$\Delta m_{31}^2/(10^{-3}\ \text{eV}^2)$	2.55	$2.25 \to 2.75$	2.55
m_1/meV			39.02
m_2/meV			39.97
m_3/meV			63.81
ϕ_{12}			0.245
ϕ_{13}			5.22
ϕ_{23}			1.46
$\langle m_{\beta\beta}\rangle/\text{eV}$			0.036
$\theta_{12}^q\ /^\circ$	13.04	$12.99 \to 13.09$	13.03
$\theta_{13}^q\ /^\circ$	0.20	$0.19 \to 0.22$	0.21
$\theta_{23}^q\ /^\circ$	2.38	$2.32 \to 2.44$	2.41
$\delta^q\ /^\circ$	68.75	$64.25 \to 73.25$	69.11
m_u/MeV	1.23	$1.08 \to 1.51$	1.23
m_c/GeV	0.620	$0.603 \to 0.637$	0.620
m_t/GeV	168	$167 \to 169$	168
m_d/MeV	2.67	$2.57 \to 2.94$	2.57
m_s/MeV	53.1	$51.61 \to 58.32$	51.7
m_b/GeV	2.84	$2.76 \to 2.87$	2.81
χ_K^2			1.05

showing that the model is in very good agreement with the experimental data.

A. "Golden" quark-lepton mass formula

A key prediction of our model comes from the fact that the charged leptons and down-quarks, both transforming as triplets of A_4, obtain their masses from the coupling with the same doublet Higgs, H_d. The flavor symmetry structure of the mass matrices M_e, and M_d in Eq. (6) implies the following relation between their masses

$$\frac{m_\tau}{\sqrt{m_\mu m_e}} \simeq \frac{m_b}{\sqrt{m_s m_d}}, \tag{35}$$

This relation has been called "golden quark-lepton mass formula" [18,41–45] and constitutes a key prediction of our model. This mass relation holds at some specific energy scale at which all other parameters of the model are evaluated. However, since this relation involves a ratio of fermion masses, its renormalization group running is significantly slower than the flow of individual fermion masses. As a result, this relation is rather "robust" in the sense that it can be considered as a good approximation over a wide energy region around a suitable reference scale of the model.

Given the precise measurements of the masses of charged lepton m_e, m_μ, m_τ and the bottom quark m_b, Eq. (35) can be interpreted as a prediction for the light quark masses m_d and m_s. These are determined by lattice simulations with larger uncertainties [46,47]. As shown in Fig. 2 it is in very good agreement with the reported values for the light quark masses at the M_Z scale [39,40]. We would like to remark the fact that not only the prediction is very close to the reported PDG values of the light quark masses, but also the updated current central value (black star) got closer to the model's prediction than before (black dot) when contrasted with references [8,9].

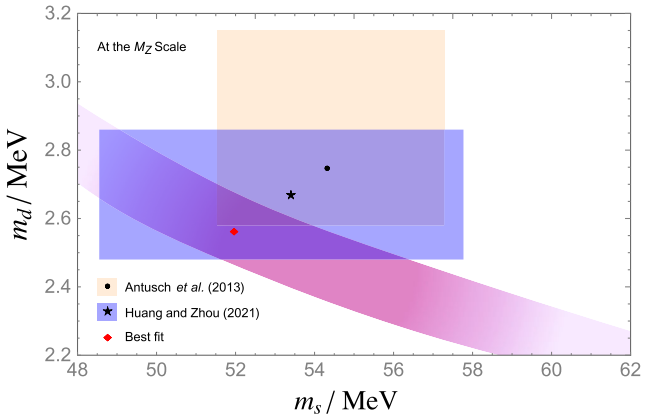

FIG. 2. In magenta we give the 3σ-predicted light quark mass m_d versus m_s at the M_Z scale, Eq. (35). In orange we display the 1σ regions in each mass from [39], and in blue the recent update in [40]. The model's best fit is denoted with a red diamond.

B. Neutrinoless double beta decay

There are other relevant observables, such as the absolute neutrino mass scale, whose value is only bounded from above by current experiments. Apart from cosmological observations [32], we have constraints from tritium beta decay endpoint measurements at Katrin [48], as well as searches for neutrinoless double beta decay [49]. The latter is a lepton number violating process and hence crucially depends on two additional physical phases [50,51] which are not included in the above discussion. These phases are present in the lepton mixing matrix but do not manifest in neutrino oscillation experiments [51].

The most convenient description of the lepton mixing matrix is the symmetrical parametrization proposed in [50] and revisited in [52]. The three physical phases are parametrized as ϕ_{12}, ϕ_{13}, and ϕ_{23}, so that the leptonic "Dirac" CP phase entering oscillations is given by

$$\delta^\ell = \phi_{13} - \phi_{12} - \phi_{23}$$

while the extra two phases are crucial to describe lepton number violating processes.

In our model neutrinos are Majorana particles, so lepton number violating processes such as $0\nu\beta\beta$ decay are expected. The associated amplitude is proportional to

$$\langle m_{\beta\beta}\rangle = |\cos^2\theta^\ell_{12}\cos^2\theta^\ell_{13} m^\nu_1 + \sin^2\theta^\ell_{12}\cos^2\theta^\ell_{13} m^\nu_2 e^{2i\phi_{12}} + \sin^2\theta^\ell_{13} m^\nu_3 e^{2i\phi_{13}}|, \quad (36)$$

Note that, as expected, $\langle m_{\beta\beta}\rangle$ only depends on the two Majorana phases, but not in the "Dirac" phase δ^ℓ.[1] In Fig. 3 we show the regions for the mass parameter $\langle m_{\beta\beta}\rangle$ characterizing the neutrinoless double beta decay amplitude, $\langle m_{\beta\beta}\rangle$. The blue region is the generally allowed one, given the current experimental determination of neutrino oscillation parameters [3], while the magenta region gives the predicted region within our model, in which all of the 19 flavor observables in both the quark and lepton sectors, Eq. (34), lie within 3-σ of their measured values. The best fit value is indicated as a red diamond, and lies somewhat below the present limit set by Kamland-Zen (36–156 meV) which is shown as the upper orange horizontal band in Fig. 3. We have also displayed the projected sensitivities for some of the next generation experiments searching for $0\nu\beta\beta$, such as LEGEND [53], SNO + Phase II [54], and nEXO [55], shown as horizontal dashed lines.

Let us now comment on Table II. As already noted, the best fit point gives $\chi^2_K = \frac{\chi^2}{K} = 1.05$ showing that indeed our model is in excellent agreement with experiment. Note also that one of the phases in the fit, $\phi^d_1 - \phi^d_2$, practically vanishes. This would suggest that a reasonable fit of the flavor parameters could be achieved even with these phase parameters fixed to vanish. Without them, one would still find a not-so-bad description, with a reduced chi-squared $\chi^2_K = 5.8$. The main tension with experiment for this case lies in the physical CP phases δ^l, δ^q, of about 3σ. This would be the price to pay for having an enhanced predictivity for other flavor observables. The vanishing of these phases could follow from the imposition of a generalized CP symmetry, in the manner described in [8].

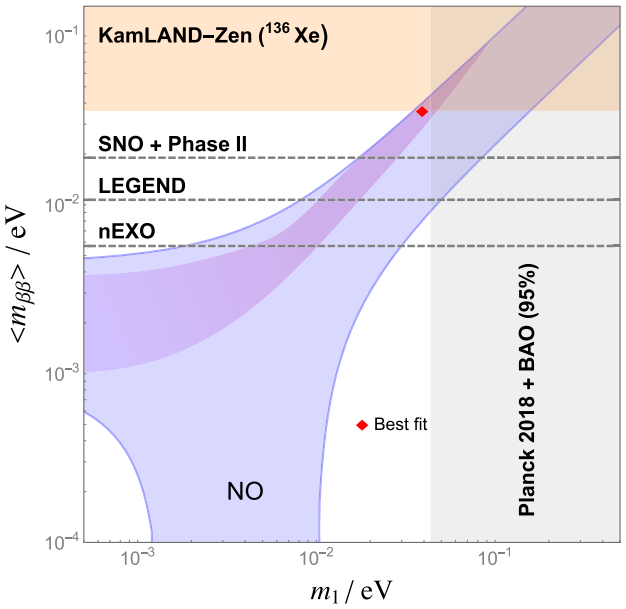

FIG. 3. Neutrinoless double beta decay mass parameter $\langle m_{\beta\beta}\rangle$ versus the mass of the lightest neutrino m_1 for the normal ordered (NO) scenario. The blue region is allowed given the current neutrino oscillation parameters [3], while the predicted magenta region is the one consistent with the masses and mixings of quarks and leptons at 3σ. The best fit point is indicated by a red diamond. The current bound on $\langle m_{\beta\beta}\rangle$ from Kamland-Zen [49] as well as future projections are shown as the upper horizontal band, and horizontal dashed lines respectively. The vertical band indicates the cosmological bound [32].

VI. DISCUSSION AND OUTLOOK

In this paper we have examined a low-scale realization of the orbifold theory of flavor proposed in [8,9]. Below compactification an A_4 family symmetry emerges naturally, providing a good description of flavor physics, see Table II. The first Kaluza-Klein excitation of the same scalar which drives family symmetry breaking and neutrino mass generation through the inverse seesaw mechanism can be identified with WIMP dark matter, see Fig. 1. The model predicts the "golden" quark-lepton mass relation, Eq. (35) and Fig. 2. Concerning neutrinos we have interesting $0\nu\beta\beta$ decay predictions shown in Fig. 3. For definiteness we have assumed the favored case of normal neutrino mass ordering. Let us also mention that our model is not necessarily meant to be a UV-complete construction. For instance, the fact

[1]In contrast to the PDG phase convention, the symmetrical parametrization provides a transparent description of $0\nu\beta\beta$ decay.

that there are three color triplets in the bulk generates 6-dimensional gauge anomalies. However, after compactification, at low energies, these anomalies cancel and the theory is consistent. One may assume that there are extra fields at high energies that cancel the anomalies at that level too [56].

All in all, our model provides an excellent global description of flavor observables both in the quark and lepton sectors, starting from first principles. Compared with the work in Refs. [8,9] the results given here correspond to a low-scale inverse seesaw mechanism and they follow from the use of updated flavor observables, such as oscillation parameters as well as recent quark mass determinations.

ACKNOWLEDGMENTS

Work supported by the Spanish grants No. PID2020–113775 GB-I00 (No. AEI/10.13039/501100011033) and Prometeo CIPROM/2021/054 (Generalitat Valenciana). O. M. is supported by Programa Santiago Grisolía (No. GRISOLIA/2020/025). C. A. V-A. is supported by the CONAHCYT Investigadoras e Investigadores por México Projects No. 749 and No. SNI 58928. The relic abundance and direct detection constraints were calculated using the micrOMEGAs package [57] at GuaCAL (Guanajuato Computational Astroparticle Lab). We thank Ignatios Antoniadis for discussions in the early phase of the work.

[1] A. B. McDonald, Nobel lecture: The sudbury neutrino observatory: Observation of flavor change for solar neutrinos, Rev. Mod. Phys. **88**, 030502 (2016).
[2] T. Kajita, Nobel lecture: Discovery of atmospheric neutrino oscillations, Rev. Mod. Phys. **88**, 030501 (2016).
[3] P. F. de Salas, D. V. Forero, S. Gariazzo, P. Martínez-Miravé, O. Mena, C. A. Ternes, M. Tórtola, and J. W. F. Valle, 2020 global reassessment of the neutrino oscillation picture, J. High Energy Phys. 02 (**2021**) 071.
[4] H. Ishimori, T. Kobayashi, H. Ohki, Y. Shimizu, H. Okada, and M. Tanimoto, Non-Abelian discrete symmetries in particle physics, Prog. Theor. Phys. Suppl. **183**, 1 (2010).
[5] N. Arkani-Hamed and M. Schmaltz, Hierarchies without symmetries from extra dimensions, Phys. Rev. D **61**, 033005 (2000).
[6] P. Chen, G.-J. Ding, A. D. Rojas, C. A. Vaquera-Araujo, and J. W. F. Valle, Warped flavor symmetry predictions for neutrino physics, J. High Energy Phys. 01 (2016) 007.
[7] P. Chen, G.-J. Ding, J.-N. Lu, and J. W. F. Valle, Predictions from warped flavor dynamics based on the T' family group, Phys. Rev. D **102**, 095014 (2020).
[8] F. J. de Anda, J. W. F. Valle, and C. A. Vaquera-Araujo, Flavour and CP predictions from orbifold compactification, Phys. Lett. B **801**, 135195 (2020).
[9] F. J. de Anda, N. Nath, J. W. F. Valle, and C. A. Vaquera-Araujo, Probing the predictions of an orbifold theory of flavor, Phys. Rev. D **101**, 116012 (2020).
[10] G. Altarelli and F. Feruglio, Tri-bimaximal neutrino mixing from discrete symmetry in extra dimensions, Nucl. Phys. **B720**, 64 (2005).
[11] G. Altarelli, F. Feruglio, and Y. Lin, Tri-bimaximal neutrino mixing from orbifolding, Nucl. Phys. **B775**, 31 (2007).
[12] G. Altarelli and F. Feruglio, Discrete flavor symmetries and models of neutrino mixing, Rev. Mod. Phys. **82**, 2701 (2010).
[13] R. N. Mohapatra and J. W. F. Valle, Neutrino mass and baryon number nonconservation in superstring models, Phys. Rev. D **34**, 1642 (1986).
[14] M. C. Gonzalez-Garcia and J. W. F. Valle, Fast decaying neutrinos and observable flavor violation in a new class of Majoron models, Phys. Lett. B **216**, 360 (1989).
[15] F. J. de Anda and S. F. King, An $S_4 \times SU(5)$ SUSY GUT of flavour in 6d, J. High Energy Phys. 07 (2018) 057.
[16] T. Kobayashi, Y. Omura, and K. Yoshioka, Flavor symmetry breaking and vacuum alignment on orbifolds, Phys. Rev. D **78**, 115006 (2008).
[17] H. Georgi and D. V. Nanopoulos, Suppression of flavor changing effects from neutral spinless meson exchange in gauge theories, Phys. Lett. **82B**, 95 (1979).
[18] S. Morisi, E. Peinado, Y. Shimizu, and J. W. F. Valle, Relating quarks and leptons without grand-unification, Phys. Rev. D **84**, 036003 (2011).
[19] R. Gonzalez Felipe, H. Serodio, and J. P. Silva, Neutrino masses and mixing in A_4 models with three Higgs doublets, Phys. Rev. D **88**, 015015 (2013).
[20] L. Nilse, Classification of 1D and 2D orbifolds, AIP Conf. Proc. **903**, 411 (2007).
[21] G. Servant and T. M. P. Tait, Is the lightest Kaluza-Klein particle a viable dark matter candidate?, Nucl. Phys. **B650**, 391 (2003).
[22] F. Burnell and G. D. Kribs, The abundance of Kaluza-Klein dark matter with coannihilation, Phys. Rev. D **73**, 015001 (2006).
[23] S. Arrenberg, L. Baudis, K. Kong, K. T. Matchev, and J. Yoo, Kaluza-Klein dark matter: Direct detection vis-a-vis LHC, Phys. Rev. D **78**, 056002 (2008).
[24] K. Kong and K. T. Matchev, Precise calculation of the relic density of Kaluza-Klein dark matter in universal extra dimensions, J. High Energy Phys. 01 (2006) 038.
[25] P. V. Dong, D. T. Huong, F. S. Queiroz, J. W. F. Valle, and C. A. Vaquera-Araujo, The dark side of flipped trinification, J. High Energy Phys. 04 (2018) 143.
[26] K.-m. Cheung and G. L. Landsberg, Kaluza-Klein states of the Standard Model gauge bosons: Constraints from high energy experiments, Phys. Rev. D **65**, 076003 (2002).

[27] R. Barbieri, A. Pomarol, R. Rattazzi, and A. Strumia, Electroweak symmetry breaking after LEP-1 and LEP-2, Nucl. Phys. **B703**, 127 (2004).

[28] N. Deutschmann, T. Flacke, and J. S. Kim, Current LHC constraints on minimal universal extra dimensions, Phys. Lett. B **771**, 515 (2017).

[29] N. Ganguly and A. Datta, Exploring non minimal universal extra dimensional model at the LHC, J. High Energy Phys. 10 (2018) 072.

[30] G. Arcadi, M. Lindner, Y. Mambrini, M. Pierre, S. Profumo, and F. S. Queiroz, The waning of the WIMP? A review of models, searches, and constraints, Eur. Phys. J. C **78**, 203 (2018).

[31] J. A. Casas, D. G. Cerdeño, J. M. Moreno, and J. Quilis, Reopening the Higgs portal for single scalar dark matter, J. High Energy Phys. 05 (**2017**) 036.

[32] N. Aghanim *et al.* (Planck Collaboration), Planck 2018 results. VI. Cosmological parameters, Astron. Astrophys. **641**, A6 (2020); **652**, C4(E) (2021).

[33] J. Aalbers *et al.* (LUX-ZEPLIN Collaboration), First Dark Matter Search Results from the LUX-ZEPLIN (LZ) Experiment, Phys. Rev. Lett. **131**, 041002 (2023).

[34] J. Billard *et al.*, Direct detection of dark matter—APPEC committee report, Rep. Prog. Phys. **85**, 056201 (2022).

[35] C. E. Aalseth *et al.* (DarkSide-20k Collaboration), DarkSide-20k: A 20 tonne two-phase LAr TPC for direct dark matter detection at LNGS, Eur. Phys. J. Plus **133**, 131 (2018).

[36] M. Schumann, L. Baudis, L. Bütikofer, A. Kish, and M. Selvi, Dark matter sensitivity of multi-ton liquid xenon detectors, J. Cosmol. Astropart. Phys. 10 (2015) 016.

[37] Y. Meng *et al.* (PandaX-4T Collaboration), Dark Matter Search Results from the PandaX-4T Commissioning Run, Phys. Rev. Lett. **127**, 261802 (2021).

[38] E. Aprile *et al.* (XENON Collaboration), Dark Matter Search Results from a One Ton-Year Exposure of XENON1T, Phys. Rev. Lett. **121**, 111302 (2018).

[39] S. Antusch and V. Maurer, Running quark and lepton parameters at various scales, J. High Energy Phys. 11 (2013) 115.

[40] G.-y. Huang and S. Zhou, Precise values of running quark and lepton masses in the Standard Model, Phys. Rev. D **103**, 016010 (2021).

[41] S. F. King, S. Morisi, E. Peinado, and J. W. F. Valle, Quark-lepton mass relation in a realistic A_4 extension of the standard model, Phys. Lett. B **724**, 68 (2013).

[42] S. Morisi, M. Nebot, K. M. Patel, E. Peinado, and J. W. F. Valle, Quark-lepton mass relation and CKM mixing in an A4 extension of the minimal supersymmetric Standard Model, Phys. Rev. D **88**, 036001 (2013).

[43] C. Bonilla, S. Morisi, E. Peinado, and J. W. F. Valle, Relating quarks and leptons with the T_7 flavour group, Phys. Lett. B **742**, 99 (2015).

[44] C. Bonilla, J. M. Lamprea, E. Peinado, and J. W. F. Valle, Flavour-symmetric type-II Dirac neutrino seesaw mechanism, Phys. Lett. B **779**, 257 (2018).

[45] M. Reig, J. W. F. Valle, and F. Wilczek, SO(3) family symmetry and axions, Phys. Rev. D **98**, 095008 (2018).

[46] R. Workman *et al.* (Particle Data Group), Review of particle physics, Prog. Theor. Exp. Phys. **2022**, 083C01 (2022).

[47] Y. Aoki *et al.* (Flavour Lattice Averaging Group (FLAG) Collaboration), FLAG review 2021, Eur. Phys. J. C **82**, 869 (2022).

[48] M. Aker *et al.*, First direct neutrino-mass measurement with sub-eV sensitivity, Nat. Phys. **18**, 160 (2022).

[49] S. Abe *et al.* (KamLAND-Zen Collaboration), First Search for the Majorana Nature of Neutrinos in the Inverted Mass Ordering Region with KamLAND-Zen, Phys. Rev. Lett. **130**, 051801 (2023).

[50] J. Schechter and J. W. F. Valle, Neutrino masses in $SU(2) \times U(1)$ theories, Phys. Rev. D **22**, 2227 (1980).

[51] J. Schechter and J. W. F. Valle, Neutrino oscillation thought experiment, Phys. Rev. D **23**, 1666 (1981).

[52] W. Rodejohann and J. W. F. Valle, Symmetrical parametrizations of the lepton mixing matrix, Phys. Rev. D **84**, 073011 (2011).

[53] N. Abgrall *et al.* (LEGEND Collaboration), The large enriched germanium experiment for neutrinoless double beta decay (LEGEND), AIP Conf. Proc. **1894**, 020027 (2017).

[54] S. Andringa *et al.* (SNO + Collaboration), Current status and future prospects of the SNO + experiment, Adv. High Energy Phys. **2016**, 6194250 (2016).

[55] J. Albert *et al.* (nEXO Collaboration), Sensitivity and discovery potential of nEXO to neutrinoless double beta decay, Phys. Rev. C **97**, 065503 (2018).

[56] B. A. Dobrescu and E. Poppitz, Number of Fermion Generations Derived from Anomaly Cancellation, Phys. Rev. Lett. **87**, 031801 (2001).

[57] G. Bélanger, F. Boudjema, A. Goudelis, A. Pukhov, and B. Zaldivar, micrOMEGAs5.0: Freeze-in, Comput. Phys. Commun. **231**, 173 (2018).